Progress In Electromagnetics Research Letters, Vol. 111, 93–102, 2023

High Sensitivity Passive Wireless Humidity Sensor Based on Polyvinyl Alcohol

Bo Wang*, Fei Gao, Youwei Li, Ke Wang, and Shengli Cao

Abstract—A low cost and compact chipless Radio Frequency Identification (RFID) humidity sensor with the size of $18 * 18 * 0.5\,\text{mm}^3$ is designed for environmental humidity monitor. The sensor consists of a circular resonator and a rectangular substrate, which utilizes the polyvinyl alcohol (PVA) humidity sensitive material for relative humidity (RH) sensing. The PVA humidity sensitive material covers the sensor surface. The working principle of the sensor is that the change of environmental humidity results in the changing of dielectric constant of PVA and thus shifting of the resonant frequency of the sensor. The real-time humidity can be observed by monitoring the resonant frequency. The simulation results show that the humidity sensing range of the designed humidity sensor is 21.9%RH $\sim$ 52.5%RH, corresponding to the resonant frequency range of the sensor from 2.76 GHz to 2.51 GHz with the total offset 250 MHz. The maximum humidity sensitivity was 23.08 MHz/%RH within the monitoring range. The designed humidity sensor has the advantages of low cost, compact and simple structure, which is suitable for humidity monitoring in various complex environments.

1. INTRODUCTION

Thanks to the development of Internet of things technology, Radio Frequency Identification (RFID) technology has been widely used. It is a very convenient technology. On the one hand, it can realize two-way wireless communication, and on the other hand, it improves the reading efficiency and longer reading distance of tags. Humidity sensors have been applied in many fields, such as logistics monitoring, aerospace, medical field, and environmental monitoring [1]. According to the measurement principle and method, the traditional humidity sensor can be divided into capacitance type [2–4], resistance type [5, 6], gravity measurement type, and microwave type. Integrating sensing technology and RFID technology, a new type of humidity sensor based on RFID is proposed as an important part of the Internet of things [7].

At present, chipless RFID humidity sensor is widely favored by the market because of its simple overall structure, low production cost, real-time monitoring of humidity changes, and low energy consumption in operation. At the same time, the main research direction of researchers is to explore more new humidity sensor structures [8–10] and humidity sensitive materials [11–13]. [14–16] have successfully integrated the humidity sensing function in RF chip, which has the characteristics of good stability and low power consumption, but there are problems such as high production cost and complex manufacturing process of the chip. A slotted scattered structure was fabricated on an FR4 substrate by slotted etching technique in [17], and the sensing unit for sensing humidity changes consists of silicon nanowires deposited on the slit surface. In [18], a bending humidity sensing structure with a size of $20 * 17.6\,\text{mm}^2$ was proposed, and a thin polyimide material was used as the sensitive material. The RFID tag was implemented on Taconic TLX-0 with a working bandwidth of 2.62 GHz. [19] designed a dual-polarized sensing tag based on a ring slot antenna element, which worked at two closely spaced

Received 6 June 2023, Accepted 11 July 2023, Scheduled 18 July 2023
* Corresponding author: Bo Wang (wangbo_chen@126.com).
The authors are with the School of Automation, Xi'an University of Posts and Telecommunications, Xi'an 710121, China.

resonant frequencies and used PVA for humidity sensing at the same time, which can be used to monitor the relative humidity in sealed packaged food. The humidity sensor proposed in [20] is used to monitor the aging problem of building structure. It adopts MEGTRON6 substrate and L-shaped resonant unit, which has a simple structure but a large size. Similarly, in some literatures, the large size of humidity sensor causes some difficulties in the use process, such as $42 * 17\,\text{mm}^2$ [21], $29 * 29\,\text{mm}^2$ [22], $23 * 23\,\text{mm}^2$ [23]. It can be seen that the sensor will be developed in the direction of miniaturized and low profile in the future.

With the development of printing technology, paper base has been paid more and more attention. [24] printed a Logic Circuit (LC) structure on packaging paper to realize the production of humidity sensor, and the frequency offset reached 16.6% within the test range. Although its sensitivity performance was high, its working frequency was low, and the identification distance was short, which has been the problem of this sensor. [25–27] also used paper as the substrate, mainly with the help of the water absorption of the paper substrate. However, when the paper is in high humidity, this relationship is nonlinear and will eventually affect the absorption peak in the Radar Cross Section (RCS) curve.

To sum up, the rigid substrate of humidity sensor has the advantage of not easy to be damaged. At the same time, the circular resonant structure is applied to the monitoring of environmental humidity, and the surface of the sensor is covered by polyvinyl alcohol to make wireless passive RFID sensor. On the one hand, the application of this structure makes the maximum use of the substrate area. On the other hand, the circular structure also makes the resonator compact. It solves the problems of low sensitivity, large size, and poor resonance characteristics of the current humidity sensor. The size of the humidity sensor is only $18 * 18 * 0.5\,\text{mm}^3$, and the humidity detection range is from 21.9%RH to 52.5%RH. It has the characteristics of miniaturization, low profile, and simple structure, and its maximum sensitivity can reach 23.08 MHz/%RH, which has good humidity detection ability for the target environment.

The rest of the paper is organized as follows. In Section 2, the working principle of the humidity sensor is introduced, and the advantages of the circular ring resonator are analyzed. At the same time, the distribution of the current on the surface of the sensor and the characteristics of PVA are described in detail. In Section 3, the method used in the simulation experiment is simply explained. The simulation results are elaborated, and the simulation data are analyzed. Section 4 summarizes the results of the paper and introduces future research directions and application scenarios.

2. SENSOR DESIGN

2.1. Humidity Sensor Structure

In this paper, a chipless RFID humidity sensor based on a circular ring resonant structure is proposed. The circular ring resonant structure is on a Rogers RO4003 dielectric substrate, and the substrate surface is covered with a humidity sensitive material PVA film to realize the humidity detection function. Fig. 1 shows the profile structure of the humidity sensor with three layers. The white layer at the top

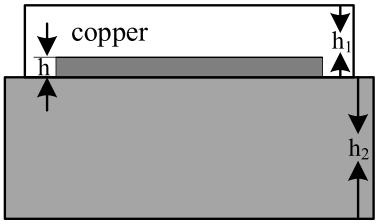

Figure 1. Profile of humidity sensor structure.

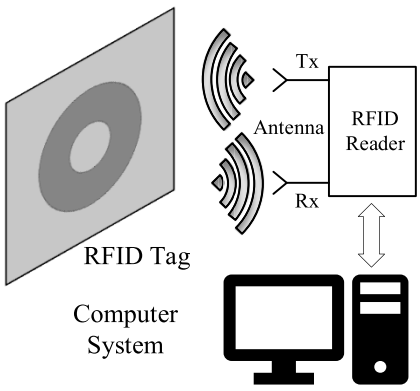

Figure 2. Working principle of RFID system.

is composed of PVA film with a thickness of h_1. The intermediate layer below uses copper as the RF conduction part of the resonator, and the thickness is h. Copper is widely used as a cheap and easy to work metal. The bottom layer uses the common Rogers RO4003 as the base, with a dielectric constant of 3.38 and a thickness of h_2.

Figure 2 shows the working principle of the RFID system and some key system components, mainly composed of RFID reader, sensor, and computer system. When the reader's transmitting antenna transmits electromagnetic waves to the surface of the sensor, at the same time, the receiving antenna will receive electromagnetic waves reflected from the surface of the sensor with a specific resonant frequency. Data processing and analysis are carried out with the help of computer processing systems [28].

2.2. Circular Ring Resonator

The tag antenna of humidity sensor adopts a circular resonant structure, which has two main advantages. 1) In terms of structure, the ring resonator is simple and symmetrical, easy to process, can maximize the use of substrate area, and can easily change its resonance value by adjusting the line width and radius of the ring structure. 2) In terms of performance, the current distribution of the ring resonator is concentrated and has good resonance characteristics [29], which can meet the performance requirements of the humidity sensor. Fig. 3 is the top view of the humidity sensor, in which the substrate width is represented by L, the ring linewidth represented by W, and R is the radius of the outer circle.

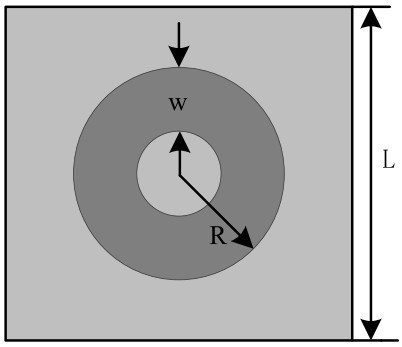

Figure 3. Top view of the humidity sensor.

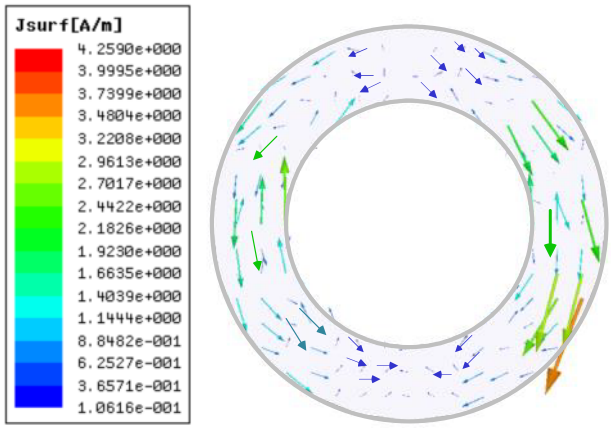

Figure 4. Current distribution of circular ring resonator.

When the circular ring structure distributed on the substrate is excited by electromagnetic waves, the resonant current appears on the metal surface and is symmetrically distributed, and the current direction flows from top to bottom. Fig. 4 shows the current distribution diagram of the circular ring resonator. At this time, the two open circuit points on the ring form a standing wave form, which can be regarded as two half wave dipoles bent in parallel. In [30], an important factor affecting the circular ring resonator was studied: the width w of the circular ring structure. On the one hand, the appropriate width w is selected to obtain the best resonance; on the other hand, the inner space of the ring is rationally arranged. At this time, formula (1) can be used to calculate the resonant frequency of the ring resonance [31].

$$f_r = \frac{c}{2 \cdot \pi \cdot R} \sqrt{\frac{2}{\varepsilon_r + 1}} \tag{1}$$

Here, c represents the speed of light in vacuum, f_r the resonant frequency of the tag, R the outer radius of the ring, and ε_r the relative dielectric constant of the substrate. According to [31], this formula temporarily ignores the thickness of the substrate.

Usually, quality factor Q is used as one of the performance indicators of the sensor. The general rule is that the sharper the trough or peak of the resonance is, the greater the quality factor Q is,

which represents the better reliability of the sensor. The quality factor Q of the sensor is calculated as follows [32]:

$$Q_d = \frac{1}{\tan\delta} \tag{2}$$

$$\frac{1}{Q} = \frac{1}{Q_d} + \frac{1}{Q_r} + \frac{1}{Q_c} \tag{3}$$

Copper is a good conductive metal, so copper conductor also has low conduction loss ($1/Q_c$) and very low radiation loss ($1/Q_r$). From formula (2), it can be seen that the tangent value of loss is inversely proportional to the quality factor Q_d, that is, the smaller $\tan\delta$ is, the larger Q_d is. Rogers RO4003 ($\varepsilon = 3.38$, $\tan\delta = 0.0027$) microwave board has a smaller loss tangent value than the commonly used FR4 ($\varepsilon = 4.6$, $\tan\delta = 0.025$) and paper ($\varepsilon = 3$, $\tan\delta = 0.0707$), theoretically, a larger value of quality factor Q which can be calculated from formula (3).

2.3. Hygroscopic Mechanism

The chipless RFID humidity sensor consists of a label and a humidity sensitive material covering the surface. The working principle of the humidity sensor is as follows: when the relative humidity in the environment changes, the dielectric constant of the humidity sensitive material covering the surface of the substrate changes accordingly. When the electromagnetic wave is used to stimulate the humidity sensor, regular deviation of the resonant frequency is observed. Therefore, the one-to-one correspondence between the environmental relative humidity and the resonant frequency of the sensor is established, and the corresponding environmental relative humidity can be known by identifying the resonant frequency of the sensor.

PVA (polyvinyl alcohol) is selected as the humidity sensitive material of the chipless RFID humidity sensor. Fig. 5 shows the molecules of PVA. A large number of hydroxyl groups are the main reason for its water absorption. Water molecules are rapidly diffused into the polymer matrix by PVA film through chemical adsorption and physical adsorption. At this time, the real part of the dielectric constant of PVA film ε_r will correspondingly decrease or increase with the change of ambient humidity [33]. Finally, it will change the real part of the effective dielectric constant ε_{reff} of the humidity sensor structure, where ε_{reff} can be calculated by formula (4) [34]:

$$\varepsilon_{reff} = 1 + q_1(\varepsilon_{sub} - 1) + q_2(\varepsilon_r - 1) \tag{4}$$

where q_1 and q_2 are constants related to the structural parameters of the resonator, and ε_{sub} and ε_r are the relative permittivity of the substrate and PVA film, respectively.

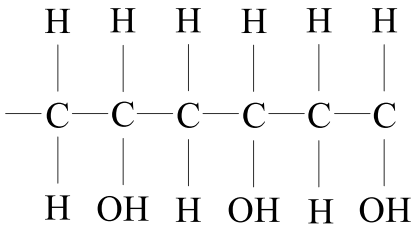

Figure 5. PVA molecular formula.

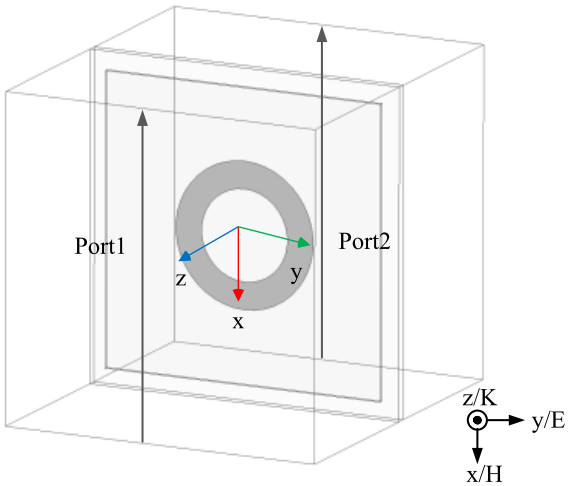

Figure 6. Simulation model of humidity sensor.

Water molecules are rapidly diffused into the polymer matrix through adsorption and absorption. Compared with hydrophobic polymers such as polyimide, the PVA based humidity sensor has higher sensitivity and faster response time [35]. In [36], it is pointed out that the permittivity of PVA is about 1.6 in a low humidity environment, but it can rapidly increase to about 80 in a high humidity environment. In [37], the dielectric constants of PVA at different humidities in the 1–10 GHz frequency band were calculated, and the dielectric constants of PVA at 2 GHz and 3 GHz were shown in Table 1.

Table 1. The electrical constant of PVA varies with different relative humidity.

%RH	21.9	29.1	35.6	44.7	52.5	64	69.5	80.4	90.9	94
2 GHz	5.06	5.08	5.18	5.38	6.2	7.7	8.6	15	29	41
3 GHz	5.12	5.14	5.21	5.41	6.18	7.5	8.4	14	27	38

3. SIMULATION ANALYSIS

Combined with the above conclusions, the radio frequency simulation software HFSS is used to model the humidity sensor. A perfect magnetic conductor (PMC) boundary is set on the surface perpendicular to the X-axis, and a perfect electric conductor (PEC) boundary is set on the surface perpendicular to the Y-axis. The two boundary surfaces are perpendicular to each other. Finally, the electromagnetic wave propagates along the Z-axis direction. Then the humidity sensing mechanism of the humidity sensitive material layer is simulated. A thin layer of 0.2 mm is added to the dielectric substrate to approximate the humidity sensing process of PVA, and the value of the dielectric constant of the sensitive layer is changed to replace the change process of the relative humidity in the environment. The simulation model of humidity sensor finally constructed is shown in Fig. 6.

The width of ring resonator affects the resonant frequency dramatically [30]. Different from [30], the proposed sensor consists of a ring resonator covered by PVA material. Thus, the simulation between the width and resonator frequency is given in Fig. 7. It is clearly shown that the resonant frequency shifts largely with increasing the width beyond 12 mm and relatively small among 14–20 mm. It is demonstrated that the resonator frequency can be adjusted by the width of the ring.

Figure 8 shows that the PVA dielectric constant parameter is set to 5.06 (21.9%RH), 5.08 (29.1%RH), 5.18 (35.6%RH), 5.38 (44.7%RH) and 6.2 (52.5%RH). The simulation curve shifts regularly in the frequency range of 2.51 GHz $\sim$ 2.76 GHz. When the permittivity of PVA is 5.06, the resonant frequency is 2.76 GHz. When PVA dielectric constant is 6.2, the resonant frequency is 2.51 GHz. The

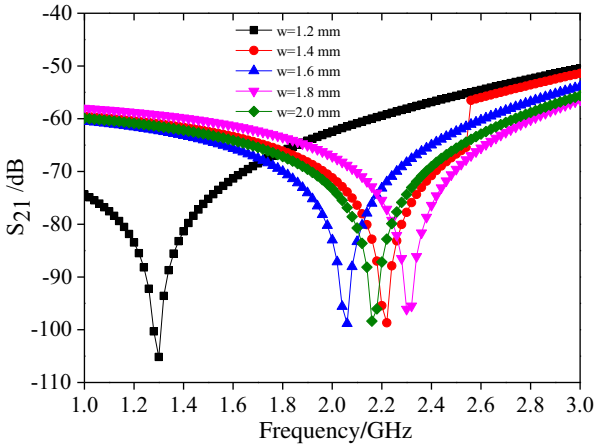

Figure 7. The width of ring w versus S_{21}.

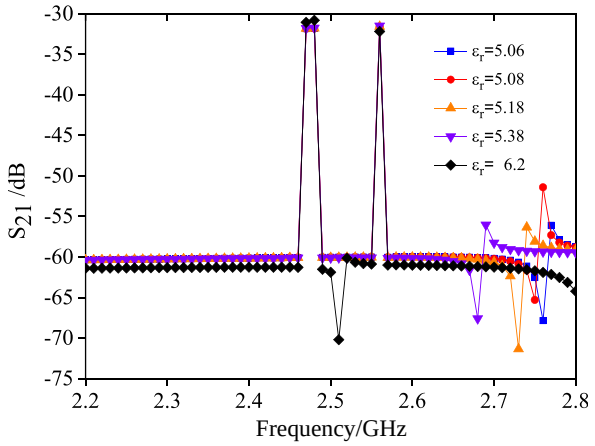

Figure 8. Variation of sensor resonant frequency under different dielectric constants.

width of the ring is $w = 1.5\,\text{mm}$, and the radius of the outer circle is $R = 4\,\text{mm}$. The simulation results show that the dielectric constant of PVA increases; the resonant frequency shifts regularly to the left; and the total offset reaches 250 MHz. The resonant frequency offset of the designed humidity sensor is obvious, and the resonant amplitude is basically the same, which is conducive to identifying the change of relative humidity in the environment. The water absorption of PVA film under different humidity conditions was measured in [36]. The experiment proved that the water absorption capacity of PVA film under low humidity conditions was far less than that under high humidity conditions, which was also the reason that the resonance frequency offset in Fig. 8 gradually increased.

Figure 9(a) shows the relationship between the permittivity of polyvinyl alcohol and the resonant frequency of the sensor. The resonant frequency points and the permittivity in Fig. 8 are extracted, and the relationship between the resonant frequency and dielectric constant is monotonically decreasing. According to [37], the variation of permittivity of polyvinyl alcohol with relative humidity is shown in Fig. 9(b). The data in Fig. 9(a) and Fig. 9(b) are associated with extracting relative humidity and resonant frequency, as shown in Fig. 10. In order to match the good linearity of the sensor, linear fitting of the sensor is carried out in two working frequency bands, and the final fitting formulas are as follows:

$$RH_{r1} = 161.27 - 43.33f \; (2.51 \leq f < 2.69) \tag{5}$$

$$RH_{r2} = -2.5 * 10^4 + 1.87 * 10^4 f - 3.49 * 10^3 f^2 \; (2.69 < f \leq 2.76) \tag{6}$$

where f represents the resonant frequency of the sensor, and RH_{r1} and RH_{r2} respectively represent the

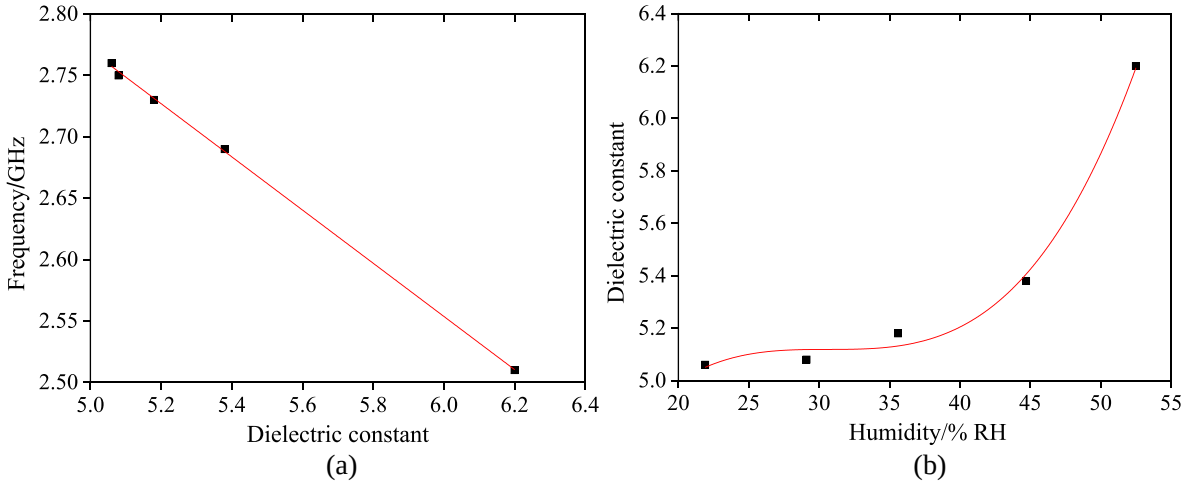

Figure 9. (a) Relation between resonant frequency and dielectric constant; (b) Relationship between dielectric constant and relative humidity.

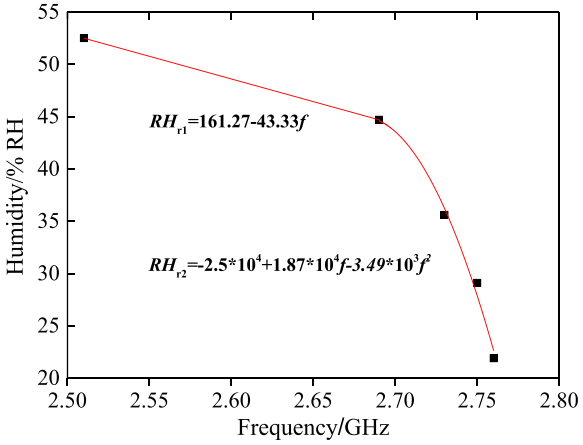

Figure 10. Relation between relative humidity and resonant frequency.

relative humidity at the corresponding frequency. It is known that the monotone decreasing relationship between the relative humidity and resonant frequency of the sensor is shown in the two frequency bands, which indicates the feasibility of the working principle of the chipless RFID humidity sensor and proves that monitoring the resonant frequency of the sensor can realize the monitoring of the ambient temperature.

In order to characterize the performance of the humidity sensor, the concept of average sensitivity η [37] is introduced. The mathematical meaning of average sensitivity is the absolute value of the reciprocal slope of the relative humidity curve changing with the resonant frequency. As shown in formula (7)

$$\eta = \frac{|f_1 - f_2|}{|RH_1 - RH_2|} \tag{7}$$

In Formula (7), the relative humidity values of the adjacent phase are expressed as RH_1 and RH_2, respectively, and the frequencies corresponding to the humidity are f_1 and f_2. The final average sensitivity calculation results are shown in Table 2. Analysis showed that the sensitivity was low when it was lower than 35.6%RH, and gradually increased with the increase of relative humidity, which increased from 44.7%RH to 52.5%RH, and the calculated sensitivity reached 23.08 MHz/%RH.

Table 2. 12.3%RH–52.5%RH humidity sensitivity η.

%RH	21.9	29.1	35.6	44.7	52.5
η	–	1.389	3.077	4.396	23.08

Table 3 shows the performance comparison between the humidity sensor in this work and other passive and chipless humidity sensors. Although the sensing range of the humidity sensor in this paper is only 21.9%RH–52.5%RH, its smaller size and greater sensitivity have good performance. The backscattered signal of the reference signal and the sensing signal are integrated into the antenna, which is one reason for the smaller size of the tag.

Table 3. Comparison of humidity sensor parameters.

Reference	Fabrication technology	Sensitive materials	Area/cm^2	Sensitivity /(MHz/%RH)	Range/%RH
This paper	Patch	PVA	3.24	23.08	$21.9 \sim 52.5$
Ref. [17]	Etch	Si nanowires	16	3.58	$30 \sim 90$
Ref. [18]	Patch	Kapton	3.52	2.14	$30 \sim 100$
Ref. [19]	Etch	PVA	7.55	–	$33 \sim 85$
Ref. [24]	Print	Paper	16	–	$20 \sim 90$

4. CONCLUSIONS

This paper carried out an in-depth research in the field of humidity sensor and designed a chipless RFID humidity sensor based on a circular ring resonant structure. Circular metal copper is distributed on the surface of the square substrate and covered by PVA humidity sensitive film.

1) The development status and wide application requirements of the current humidity sensor are expounded. The working principle of the RFID humidity sensor and the water absorption principle of PVA film are introduced. The current characteristics of the ring resonator are analyzed.

2) HFSS is used to complete the overall simulation work. By changing the dielectric constant of PVA film and the change process of environmental humidity, it is proved that there is a linear relationship between relative humidity and resonant frequency: relative humidity increases; resonant frequency decreases; and the piecewise fitting formula is calculated.

3) The sensor realizes low cost and miniaturized design. The overall size is $18 * 18 * 0.5\,\mathrm{mm}^3$; the relative humidity monitoring range is 21.9%RH $\sim$ 52.5%RH; the corresponding resonant frequency offset is 250 MHz; and the humidity sensitivities under different relative humidities are compared. The maximum humidity sensitivity η can reach 23.08 MHz/%RH, which has good humidity detection accuracy and can realize humidity detection in complex environments.

The key research direction in the future is how to expand the humidity sensing range and explore the influence of humidity sensing film thickness on the sensitivity so as to improve the performance of humidity sensor.

ACKNOWLEDGMENT

This research was funded by the Youth Science Foundation of the National Natural Science Foundation of China (No. 12204373) and Natural Science Basic Research Program of Shaanxi (No. 2023-JC-QN-0002).

REFERENCES

1. Jeong, H., Y. Noh, and D. Lee, "Highly stable and sensitive resistive flexible humidity sensors by means of roll-to-roll printed electrodes and flower-like TiO_2 nanostructures," *Ceramics International*, Vol. 45, No. 1, 985–992, 2019.
2. Bi, H., K. Yin, X. Xie, J. Ji, S. Wan, L. Sun, and M. S. Dresselhaus, "Ultrahigh humidity sensitivity of graphene oxide," *Scientific Reports*, Vol. 3, No. 1, 2714, 2013.
3. Liu, J. H., L. D. Du, J. Jin, Z. Fang, and Z. Zhao, "Improvement of the microcapacitive humidity sensor by the package optimization," *Micro & Nano Letters*, Vol. 15, No. 3, 145–148, 2020.
4. Kim, J., J. H. Cho, H. M. Lee, and S. M. Hong, "Capacitive humidity sensor based on carbon black/polyimide composites," *Sensors*, Vol. 21, No. 6, 1947, 2021.
5. Smith, A. D., K. Elgammal, F. Niklaus, A. Delin, A. C. Fischer, S. Vaziri, and M. C. Lemme, "Resistive graphene humidity sensors with rapid and direct electrical readout," *Nanoscale*, Vol. 7, No. 45, 19099–19109, 2015.
6. Packirisamy, M., I. Stiharu, X. Li, and G. Rinaldi, "A polyimide based resistive humidity sensor," *Sensor Review*, Vol. 25, No. 4, 271–276, 2005.
7. Borgese, M., F. A. Dicandia, F. Costa, S. Genovesi, and G. Manara, "An inkjet printed chipless RFID sensor for wireless humidity monitoring," *IEEE Sens. J.*, Vol. 17, No. 15, 4699–4707, 2017.
8. Abbasi, Z., M. Baghelani, and M. Daneshmand, "Zero power consumption chipless distant microwave moisture sensor for smart home applications," *Proc. IEEE Sensors*, 1–4, Montreal, Canada, October 2019.
9. Bagchi, S., A. Shakouri, R. Rahimi, N. Raghunathan, and J. F. Waimin, "Battery-less wireless chipless sensor tag for subsoil moisture monitoring," *IEEE Sens. J.*, Vol. 21, No. 5, 6071–6082, 2020.
10. Yao, Y., H. Zhang, J. Sun, W. Y. Ma, L. Li, W. Z. Li, and J. Du, "Novel QCM humidity sensors using stacked black phosphorus nanosheets as sensing film," *Sensors Actuat. B: Chem.*, Vol. 244, 259–264, 2017.
11. Lu, D., Y. Zheng, A. Penirschke, and R. Jakoby, "Humidity sensors based on photolithographically patterned PVA films deposited on SAW resonators," *IEEE Sens. J.*, Vol. 16, No. 1, 13–14, 2015.
12. Zhang, Y., Y. Chen, Y. Zhang, H. Cong, B. Fu, S. Wen, and S. Ruan, "A novel humidity sensor based on NH2-MIL-125(Ti) metal organic framework with high responsiveness," *J. Nanopart. Res.*, Vol. 15, 1–6, 2003.
13. Le, X. H., X. Y. Wang, J. T. Pang, Y. J. Liu, B. Fang, Z. Xu, C. Gao, Y. Xu, and J. Xie, "A high performance humidity sensor based on surface acoustic wave and graphene oxide on AlN/Si layered structure," *Sensors Actuat. B: Chem.*, Vol. 255, 2454–2461, 2018.
14. Cirmirakis, D., A. Demosthenous, N. Saeidi, and N. Donaldson, "Humidity-to-frequency sensor in CMOS technology with wireless readout," *IEEE Sens. J.*, Vol. 13, No. 3, 900–908, 2012.

15. Tan, Z. C., R. Daamen, A. Humbert, Y. V. Ponomarev, Y. Chae, and M. A. P. Pertijs, "A 1.2-V 8.3-nJ CMOS humidity sensor for RFID applications," *IEEE J. Solid-St. Circ.*, Vol. 48, No. 10, 2469–2477, 2013.
16. Deng, F. M., Y. G. He, C. L. Zhang, and W. Feng, "A CMOS humidity sensor for passive RFID sensing applications," *Sensors*, Vol. 14, No. 5, 8728–8739, 2014.
17. Deng, F. M., Y. G. He, B. Li, Y. Song, and X. Wu, "Design of a slotted chipless RFID humidity sensor tag," *Sensor Actuat. B-Chem.*, Vol. 264, 255–262, 2018.
18. Ali, A., S. I. Jafri, A. Habib, Y. Amin, and H. Tenhunen, "RFID humidity sensor tag for low-cost applications," *Appl. Comput. Electrom. Society*, Vol. 32, No. 12, 1083–1088, 2017.
19. Raju, R. and G. E. Bridges, "Radar cross section-based chipless tag with built-in reference for relative humidity monitoring of packaged food commodities," *IEEE Sens. J.*, Vol. 21, No. 17, 18773–18780, 2021.
20. Komoda, N., T. Michisaka, and M. Kondo, "Novel sensing techniques of chipless RFID sensor for infrastructure," *IEICE Commun. Expr.*, Vol. 9, No. 6, 244–249, 2020.
21. Habib, A., R. Asif, M. Fawwad, Y. Amin, J. Loo, and H. Tenhunen, "Directly printable compact chipless RFID tag for humidity sensing," *IEICE Electron. Expr.*, Vol. 14, No. 10, 20170169–20170169, 2017.
22. Sumra, Z., H. Ayesha, S. J. Anum, A. Yasar, L. Jonathan, and T. Hannu, "Dual-polarized chipless humidity sensor tag," *IEICE Electron. Expr.*, Vol. 14, No. 21, 20170926–20170926, 2017.
23. Anum Satti, J., A. Habib, H. Anam, S. Zeb, Y. Amin, J. Loo, and H. Tenhunen, "Miniaturized humidity and temperature sensing RFID enabled tags," *Int. J. RF Microw. Comput. Aided Eng.*, Vol. 28, No. 1, e2115, 2017.
24. Feng, Y., L. Xie, Q. Chen, and L. R. Zheng, "Low-cost printed chipless RFID humidity sensor tag for intelligent packaging," *IEEE Sens. J.*, Vol. 15, No. 6, 3201–3208, 2015.
25. Zeb, S., A. Habib, Y. Amin, H. Tenhunen, and J. Loo, "Green electronic based chipless humidity sensor for IoT applications," *2018 IEEE Green Technologies Conference*, 172–175, Austin, USA, April 2018.
26. Xie, M. Z., L. F. Wang, L. Dong, W. J. Deng, and Q. A. Huang, "Low cost paper-based LC wireless humidity sensors and distance-insensitive readout system," *IEEE Sens. J.*, Vol. 19, No. 12, 4717–4725, February 2019.
27. Gaspar, C., J. Olkkonen, S. Passoja, and M. Smolander, "Paper as active layer in inkjet-printed capacitive humidity sensors," *Sensors*, Vol. 17, No. 7, 1464, 2017.
28. Barman, B., S. Bhaskar, and A. K. Singh, "Spiral resonator loaded S-shaped folded dipole dual band UHF RFID tag antenna," *Microw. Opt. Technol. Lett.*, Vol. 61, No. 3, 720–726, 2019.
29. Athauda, T. and N. C. Karmakar, "The realization of chipless RFID resonator for multiple physical parameter sensing," *IEEE Internet Things*, Vol. 6, No. 3, 5387–5396, 2019.
30. Vena, A., E. Perret, and S. Tedjini, "High capaciy chipless RFID tag insensitive to the polarization," *IEEE Trans. Microwave Theory Tech.*, Vol. 60, No. 10, 4509–4515, 2012.
31. Dissanayake, T. and K. P. Esselle, "Prediction of the notch frequency of slot loaded printed UWB antennas," *IEEE Trans. Antennas Propag.*, Vol. 55, No. 11, 3320–3325, 2007.
32. Vena, A., E. Perret, and S. Tedjini, "Chipless RFID based on RF encoding particle: Realization, coding, reading system," *Remote Identification beyond RFID Set*, 171–180, ISTE Press, London, UK; Elsevier, London, UK, August 2016.
33. Kok, Y. Y., Z. Abbas, K. Khalid, and M. Z. Rahman, "Improved dielectric model for polyvinyl alcohol-water hydrogel at microwave frequencies," *Am. J. Appl. Sci.*, Vol. 7, No. 2, 270–276, 2010.
34. Gevorgian, S., L. Linner, and E. L. Kollberg, "CAD models for shielded multilayered CPW," *IEEE Trans. Microwave Theory Tech.*, Vol. 43, No. 4, 772–779, 1995.
35. Paul, D. R., "Water vapor sorption and diffusion in glassy polymers," *Macromolecular Symposia*, Vol. 138, No. 1, 13–20, WILEY-VCH Verlag GmbH & Co. KGaA, Weinheim, Germany, March 1999.
36. Sengwa, R. J. and K. Kaur, "Dielectric dispersion studies of poly (vinyl alcohol) in aqueous solutions," *Polym. Int.*, Vol. 49, No. 11, 1314–1320, 2000.

37. Lu, D., Y. Zheng, A. Penirschke, A. Wiens, and R. Jakoby, "Humidity dependent permittivity characterization of polyvinyl-alcohol film and its application in relative humidity RF sensor," *2014 44th European Microwave Conference*, 163–166, Rome, Italy, October 2014.